about 20 mb/sr for V and Cu, at this angle. The cross section drops sharply with angle, and the data indicate that in the backward hemisphere statistical processes dominate, but are several orders of magnitude smaller than the direct interaction processes in the forward hemisphere. Let us assume a conservative average differential cross section for direct interaction processes leading to (He^4, $He^{4\prime}$) events above 20-MeV excitation. From Igo's data, such a conservative cross section would be about 20 mb for these elements. Dostrovsky's emission widths may be used to compute the expected frequency of emission of the He ion by evaporation relative to the emission of other particles. At 30-MeV excitation, we find that about one in thirty total emissions will be an alpha particle. But $(20\text{ mb})\times(1/30)=0.67$ mb, and we see that the (He^4,$2He^4$) reaction through the inelastic scattering-evaporation mechanisms is likely to be highly competitive with the double evaporation mechanism, at 40 MeV.

The (He^4,$2He^4n$) reaction in vanadium and cobalt was investigated in the energy range from 35 to 41 MeV and the results are given in Table IV. At 40.8 MeV average He-ion energy a cross section of 0.61 mb was found for the V^{51} reaction and at 40.5 MeV a value of 6.2 mb for the Co^{59} reaction. This order of magnitude difference between the two cross sections can be explained on the basis of the Q values for the reactions being (-17.2 MeV) for Co^{59} and about -20.9 MeV for V^{51}, a difference of about 3.7 MeV. At 36.8 MeV, the Co^{59}(He^4,$2He^4n$) reaction has a cross section of 1.7 mb, a number much more comparable with the vanadium cross section at 40.8 MeV.

ACKNOWLEDGMENTS

The authors are grateful for the help of the Research Advisory Committee of Western Washington State College for supplying financial assistance during the study. We would like to thank Ted Morgan of the University of Washington Cyclotron Laboratory, Dr. Norton Hintz of the University of Minnesota, and Dr. Charles Waddell of the University of Southern California for arranging the bombardments.

PHYSICAL REVIEW VOLUME 131, NUMBER 4 15 AUGUST 1963

Studies of Alpha Particles from the Li^6-Li^6 Nuclear Reaction*

MINAO KAMEGAI†

Department of Physics and The Enrico Fermi Institute for Nuclear Studies, The University of Chicago, Chicago, Illinois

(Received 10 April 1963)

The reaction mechanism and the states in Be^8 in a Li^6-induced reaction $Li^6(Li^6,\alpha)Be^8 \rightarrow 3\alpha$, were studied by a double-coincidence experiment in which angles and energies of the two simultaneous alphas were recorded. The bombarding energy was 1.9 MeV. When the data are transformed to the center-of-mass system, it is shown that a mechanism in which the entire available energy is divided equally between two alphas emitted 180° apart is some 23 times more probable than one in which one of the alphas recoils from Be^8 in its ground state. There are also satellite coincidence maxima at 169° and 192°. The pattern can be interpreted as due to a cluster reaction mechanism in which Li^6 combines with a deuteron cluster to produce a state of Be^8 at 20.95 ± 0.3 MeV which is (Li^6+d)-like. The pattern is fitted best, if a Breit-Wigner probability distribution for the excited Be^8 state is assumed, by a total width of 3.4 MeV. It is estimated that the α-decay width of this state is 260 ± 90 keV. Such a mechanism has previously been suggested by Coste and Marquez, following ideas of Temmer. The angular distribution of the alpha group which leaves Be^8 in its ground state is nearly isotropic in the barycentric system. It seems that the reaction leading to the ground state of Be^8 proceeds through an intermediate compound nucleus, C^{12*}. The absolute total cross section for an intermediate stage involving the ground state of Be^8 is 5.8×10^{-29} cm²; for the 20.85 MeV state it is 13×10^{-28} cm².

I. INTRODUCTION

THIS work is an experimental study of the alpha particles from the nuclear reaction $Li^6(Li^6,\alpha)2\alpha$ as induced by Li^6 ions near 2.0-MeV kinetic energy. Figure 1 shows the energy spectrum of these alphas after transforming the data, taken by a conventional particle selection system, to the barycentric system. A similar result has been published by a group in Saclay, France[1] who studied the spectrum by an emulsion technique.

The most energetic and weakest group at 14.52 MeV arises from the alpha particles that leave the residual Be^8 nucleus in its ground state. The second group at 12.59 MeV corresponds to the first excited state of Be^8, namely, the 2^+ state. The main feature of the spectrum in Fig. 1 is an intense group which is located at

* This work was supported in part by the U. S. Atomic Energy Commission.

† Submitted in partial fulfillment of the requirements for the Ph.D. degree.

[1] M. Coste and L. Marquez, Compt. Rend. **254**, 1768 (1962).

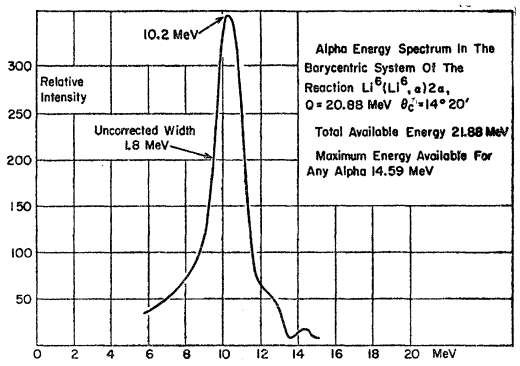

FIG. 1. The alpha-energy spectrum taken at 14°20′ (lab) and transformed to the barycentric system.

10.25±0.5 MeV. This does not represent recoil from any presently known state in Be^8. We consider three different interpretations of this group.

Hypothesis 1. Random tripartition of C^{12}: Let $P(\epsilon)$ be the probability that any one of the three alpha particles will have kinetic energy ϵ. Since the α particles are bosons, the method of analysis developed by Dalitz[2] for the disintegration of the τ meson into 3 pions is applicable. If the probability of any distribution of the three kinetic energies ϵ_1, ϵ_2, and ϵ_3 is independent of the individual values ϵ_1, ϵ_2, and ϵ_3, the result of Dalitz is

$$P(\epsilon)d\epsilon=\frac{6}{\pi T}\left(3\frac{\epsilon}{T}\right)^{1/2}\left(2-\frac{3\epsilon}{T}\right)^{1/2}d\epsilon, \qquad (1)$$

where $P(\epsilon)$ is the probability that a disintegration will occur in which one of the alphas has the energy ϵ. T is the total energy available in the barycentric system, and the range of ϵ is from 0 to $2T/3$. This distribution will be referred to as a random or isotropic breakup, showing no tendency to form a two-body intermediate. If attractive forces of a non-pair-forming type play an appreciable role in the breakup, the maximum of the above equation at $\epsilon=\frac{1}{3}T$ will be more pronounced, but will remain in the center of the distribution. Since the unknown peak in question appears off center, at $\epsilon=0.47T$, it seems that the tripartition of C^{12} does not explain this group.

Hypothesis 2. Existence of a 6.4-MeV state in Be^8: If the random three-body decay is not the predominant mode of decay, one can assume a two-stage reaction,

$$Li^6(Li^6,\alpha_1)Be^{8*} \quad \text{followed by} \quad Be^{8*}\rightarrow\alpha_2+\alpha_2'. \qquad (2)$$

If this unknown group is the α_1 from the first stage of the reaction, the spectrum suggests the existence of a 6.4 MeV state in Be^8.

Hypothesis 3. Existence of (Li^6+d)-like resonance states near 20 MeV in Be^8: If the reaction proceeds in such a way that one Li^6 captures the deuteron cluster of the other Li^6, Be^{8*} can result in states near 20 MeV which lie close to the deuteron threshold at 22.28 MeV.[3] After some rearrangement of the nucleons, dissociation into two alphas follows. This mechanism has been suggested by Coste and Marquez.[4] These secondary alpha particles have energies of approximately 10 MeV with respect to the Be^{8*} which may be in motion in the barycentric system. Using the notation given in Eq. (2), one notes that the unknown group is now primarily composed of α_2 and α_2'.

The study of double coincidences between any two alpha particles with measurement of their energies, can distinguish between the mechanisms of hypotheses 2 and 3. Double coincidences were studied over a wide range of angles in the laboratory system. In addition, the angular distribution and the total cross section of the ground-state group were measured.

II. APPARATUS AND EXPERIMENTAL PROCEDURE

A singly charged lithium-6 beam was furnished by the University of Chicago 2-MeV Van de Graaff. The ion source used has already been described by Allison and Kamegai.[5]

The kinetic energies were determined by a 90° electrostatic deflector which was described in detail in a previous publication[6] by Huberman, Kamegai, and Morrison, hereinafter referred to as HKM. The beam is deflected through 90° between two curved aluminum plates with a gap of 0.572 cm, the inner plate being maintained at a negative potential and the outer plate being grounded. The radii of curvature of these plates are 91.156 and 91.728 cm, respectively. This makes it possible to define the energy within 0.67%.

Although the ion source emits a remarkably pure lithium beam relatively free of foreign ions, a sorting magnet is used to direct the lithium-6 beam into a port with an angular deviation of $22\frac{1}{2}$°. This assures the

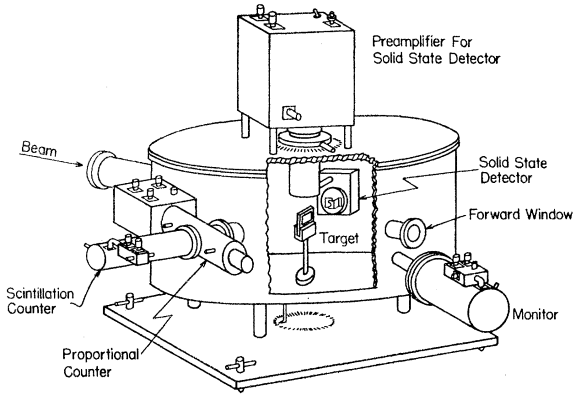

FIG. 2. Target chamber for the double-coincidence experiments.

[2] R. H. Dalitz, Phil. Mag. 44, 1068 (1953).

[3] G. M. Temmer, Bull. Am. Phys. Soc. **7**, 59 (1962).
[4] M. Coste and L. Marquez, Compt. Rend. **254**, 1768 (1962).
[5] S. K. Allison and M. Kamegai, Rev. Sci. Instr. **32**, 1090 (1962).
[6] M. N. Huberman, M. Kamegai, and G. C. Morrison, Phys. Rev. **129**, 791 (1963).

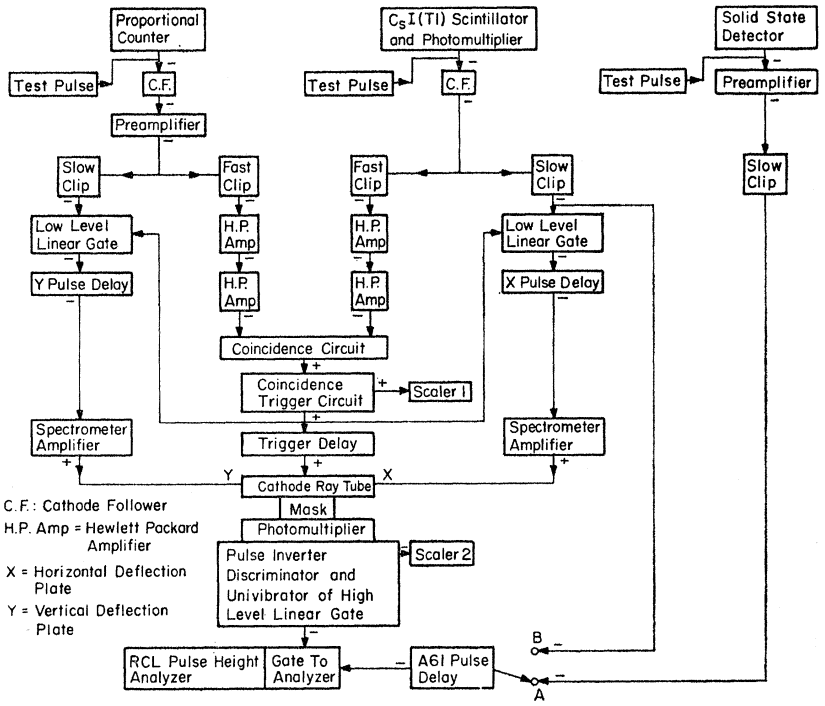

FIG. 3. Block diagram of the electronic circuits for double-coincidence measurements.

separation of the lithium-6 isotope from any lithium-7 present, and in addition, for the final experiments, the filament coating was prepared from the 99.3% enriched lithium-6 isotope produced by the Oak Ridge National Laboratory.

The target was prepared in vacuum by evaporating a piece of metallic lithium-6 isotope forming a layer approximately 1.0 mg/cm² thick on a thin aluminum backing foil of 1.24 mg/cm² thickness. For the measurement of absolute cross sections where the exact composition of the target material was required, a stable lithium compound, LiF, was used as the thick target material.

A. Angular Distributions

The target chamber for the measurement of relative differential cross sections, and the apparatus and procedure for measuring absolute cross sections have been previously described in HKM and were used without modification.

B. Coincidence Experiments

The main feature of the present experiment concerns double coincidences between the particle selection system and a solid state detector. For this purpose, a special reaction chamber was designed. Figures 2 and 3 show the sketch of the chamber and the block diagram of the electronics, respectively. The cylindrical compartment of inner radius 15.2 cm and wall thickness 0.5 cm houses a target and the solid-state detector (SSD) which can be moved 360° around the target. The particle selection system (PSS) is attached to the side of the chamber at 90° with respect to the incident beam direction. The chamber is carefully aligned so that the PSS, the target, and the SSD are coplanar. In this setup, the PSS serves only for the purpose of opening the gate to the pulse-height analyzer, and the "E_s" pulse of any particle detected by the SSD can enter the analyzer only when two particles, one responsible for the gate pulse and the other responsible for the "E_s" pulse, arrive in coincidence at the PSS and the SSD, respectively.

In testing the circuits, a single test pulse from a mercury pulse generator was branched and fed into the PSS and the SSD, and the output pulses from these systems were displayed on a dual channel scope. The "E_s" pulse from the SSD had a rise time of nearly 1 μsec and a decay time of 3 μsec, and the gate pulse from the PSS and a rise time of 2 μsec, decaying in 2 μsec after maintaining the maximum for 2 μsec. The "E_s" pulse is delayed so that both pulses reach the maximum simultaneously.

The SSD is located 7.62 cm from the target with a solid angle of 3.39×10^{-3} sr. On the other hand, the path length of the particles in the PSS is 27.78 cm, and the particles are received into a solid angle of 1.15×10^{-3} sr.

The object of the double-coincidence work is to study the angular correlation between two alpha particles from the nuclear reaction $Li^6(Li^6,\alpha_1)Be^{8*}$, $Be^{8*}\rightarrow\alpha_2+\alpha_2'$. As described in HKM the "dE/dx" and the E pulses of the PSS were displayed on an oscilloscope screen and "seen" by a phototube, the pulses from which opened a gate to the pulse-height analyzer. The spots from protons, deuterons, alphas, etc., lay on characteristic curves, and particle discrimination was achieved by masking the

oscilloscope screen so that only the desired curve was exposed. In the present coincidence measurements there was both particle selectivity and energy selectivity; only a segment of the alpha curve near the large peak being exposed. The energy range exposed for coincidence testing was from 9.55 to 10.95 MeV with an uncertainty of ± 0.7 MeV in the upper and lower limits, which included the peak at 10.25 MeV. The SSD and its circuits would register alpha particles in the range from 1 to 14 MeV.

The reference direction from which the angular positions of the two detectors are given is the direction of the beam, from left to right in Fig. 2. The angles θ_p or θ_s which are discussed represent positions of the PSS or of the SSD which correspond to angular displacements in the clockwise direction as viewed from above in Fig. 2. The positions given are always those which have been obtained by reduction of the data to the barycentric system unless specifically mentioned otherwise. Thus, Fig. 2 shows $\theta_p = 90°$ (lab) and $\theta_s = 260°$ (lab). When the angle θ_{ps} between the detectors is mentioned it is given by $(\theta_s - \theta_p)$.

The apparatus was tested by means of the known two-body reaction $p(\mathrm{Li}^7,\alpha)\alpha$. The coincidence rate is defined as the ratio of the number of coincidences to the number of alpha particles captured in the particle selection system during the same interval. With 2-MeV Li^7 projectiles on a plastic foil target, the expected coincidences appeared over a half-maximum angular range of 5° at the calculated angle.

During the experiment, the electronic drift of the apparatus and the linearity of the pulse-height analyzer were checked once a day by means of a mercury pulse generator. Also twice a day, the coincidence apparatus was checked by the following method. Referring to Fig. 3, the input to the A61 pulse delay was switched from terminal A to terminal B. As previously stated, the PSS is masked to allow only the alpha particles in an energy range 1.4 MeV wide near the maximum of the unknown peak to function as gate pulses. Hence, only this portion of the alpha spectrum can enter the pulse-height analyzer. As shown in the diagram, the scaler 2 registers the gate pulses from the photomultiplier viewing the cathode ray tube. If the gate pulses are opening the gate to the pulse-height analyzer whenever the "E_s" pulses in the allowed energy range of the alpha spectrum arrive at the analyzer, the total number of counts stored in the analyzer must equal the number of counts registered by the scaler 2. This was found to be the case without an exception.

Immediately after the test described above, the input to the A61 pulse delay was returned to terminal A, and then the experiment was performed. Therefore, for the double-coincidences experiment, the scaler 2 provided the measure of the total number of the alpha particles in the allowed range in the alpha spectrum, whereas the analyzer supplied the energy and the number of the alpha particles captured by the SSD in coincidence at various angles.

TABLE I. Reduction of coincidence data to the barycentric system.

1. PSS detector position	$\theta_p = 90°$ (lab)
2. Mean PSS energy observed (after absorption corrections)	9.93 MeV (lab)
3. PSS angle transformed	101° (c.m.)
4. Mean PSS energy transformed	10.25 (c.m.)
5. SSD coincidence detector position	$\theta_s = 290°$ (lab)
6. SSD coincident energy (corrected for absorption)	13.13 MeV (lab)
7. SSD barycentric energy	$E_s = 12.05$ MeV
8. SSD barycentric angle	$\theta_s = 281°07'$
Coincidence ratio observed	4.95×10^{-3}

III. RESULTS AND SOURCES OF ERRORS

A. Double Coincidences

The search for coincidences extended over the angular range $240° < \theta_s < 330°$ in the laboratory system, with the PSS detector fixed at 90° (lab) and an initial Li^6 laboratory energy of 1.9 MeV.

Due to the limited energy range which the PSS would accept, the reduction of its data to the barycentric system resulted in essentially a fixed barycentric angle, $\theta_p = 101°$, and the barycentric energy range 10.25 ± 0.7 MeV. The transformation of the results of a single coincidence run to the barycentric system are outlined in Table I.

The number of accidental coincidences per unit time, N_a, is given by

$$N_a = 2\tau N_s N_p ,$$

where τ is the resolving time, and N_s and N_p are the counting rates for the SSD and the PSS, respectively. In t sec, we accumulate the total accidental coincidences of

$$tN_a = 2\tau N_s (tN_p) ,$$

where tN_p is the total number of counts registered by the PSS. From the definition of the coincidence rate, the accidental coincidence rate is

$$N_a/N_p = 2\tau N_s .$$

From a study of the pulse shapes τ was taken to be 4×10^{-6} sec. The upper limit of N_s was estimated to be 200 counts per second. Thus,

$$2\tau N_s = 1.6 \times 10^{-3} .$$

However, this includes all possible energies of the particles received by the SSD and is exhibited in different channels of the pulse-height analyzer. Thus, this accidental coincident rate was apportioned among various channels to be subtracted from the counts stored in those channels, and subtracted from the observed rate.

Coincidences were rejected if the energy registered by the SSD was not compatible with the kinematically possible range determined by the energies permitted in the PSS and the angle between the two detectors. The calculation can be made without any assumptions as to a reaction mechanism since the energies ϵ_1, ϵ_2, ϵ_3, and

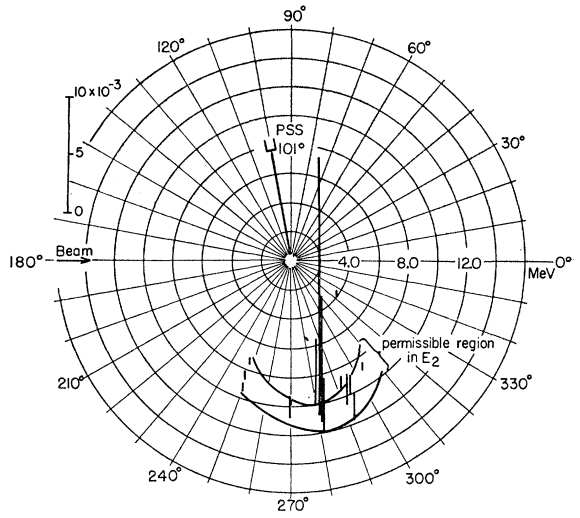

FIG. 4. Observed coincidence ratios plotted in the barycentric system. The figure may be considered three dimensional, the height of the "vertical" solid lines representing the coincidence ratios according to the scale at the upper left. Energies are plotted radially in the plane of the figure. The solid curves enclose the region of kinematically permissible energies. The PSS detector fixes the barycentric angle of one of the alphas at 101° and its energy to 10.25±0.7 MeV.

the two angles are all determined if two of the parameters, such as ϵ_1 and one angle are known.

The kinematically permissible energies were calculated as follows. Since the total available energy T is fixed and known, let ϵ_p be an alpha energy in the energy range (9.55–10.95 MeV) accepted by the PSS. The setting θ_{ps} determines the angle between the central rays accepted by the two detectors. Then,

$$\epsilon_s=\tfrac{1}{2}m\{-\tfrac{1}{2}v_p\cos\theta_{ps} \pm\tfrac{1}{2}[v_p^2\cos^2\theta_{ps}+4((T/m)-v_p^2)]^{1/2}\}^2, \quad (3)$$

TABLE II. Coincidence results.[a] The PSS detector is fixed at an angle θ_p corresponding to 101° in the barycentric system.

θ_s Angle of coincidence detector with respect to beam	θ_{ps} Angle between coincidence detectors	E_s Barycentric energy in coincidence det. (MeV) (obs)	Coincidence rate×10^3 (corrected for accidentals)
322.5	221.5	3.92	0.17
303.5	202.5	9.08	0.48
294	193	9.99	1.47
291.8	190.8	11.76	2.55
291.5	190.5	10.60	2.69
291	190	9.69	1.21
281	180	12.05	4.70
281	180	11.26	11.08
280.5	179.5	10.76	22.83
280	179	9.89	5.66
277	169	9.78	0.19
270	169	10.75	1.75
249.7	148.7	9.64	0.67
249	148	8.66	0.67
248.3	147.3	7.50	0.40

[a] For brevity, angular settings are omitted in regions where a search was made, but nothing above the accidental rate was detected.

where v_p is the mean velocity accepted by the PSS, m is the α mass, and ϵ_s is the energy accepted in the SSD in coincidences. The sum of the angles subtended by the aperture of the PSS and the SSD leads to an angular range of 5°58′; from this and the range in ϵ_p (9.55–10.95 MeV) a permissible range of ϵ_s for each setting of the SSD was calculated. The permissible energy region is indicated on Fig. 4.

In addition to the two corrections described above, the angle of multiple scattering was calculated[7] and was found to be less than 0.2° which is negligible compared to 3°46′ subtended by the solid-state detector.

The final results for the coincidence rate are shown in Table II. Figure 4 is a three-dimensional plot of the data in which the radial scale is the energy of the alpha particles at various angles, and the length of the pole indicates the coincidence rate. The scale of the coincidence rate is shown in the upper left-hand corner. The PSS is located at 90° in the laboratory system which corresponds to 101° in the barycentric system.

B. Expected Coincidence Rates According to the Various Hypotheses

In this section, the expected coincidence rates for the three hypotheses previously presented are calculated.

1. Tripartition of C^{12}

Dalitz[2] has pointed out that a system which disintegrates into three identical bosons can be represented by a point within an equilateral triangle whose altitude is equal to T, the total amount of energy available for transformation into kinetic energies. This can be understood if one notes that the sum of the normals from any point to the three sides of the triangle is equal to the altitude. Figure 5 is the Dalitz triangle. Since the maximum energy that each particle can have is $\frac{2}{3}T$, the points must be enclosed within a circle of radius $\frac{1}{3}T$. For a random three-body decay with no interaction among them, Dalitz has shown that the configuration points are uniformly distributed throughout the circle.

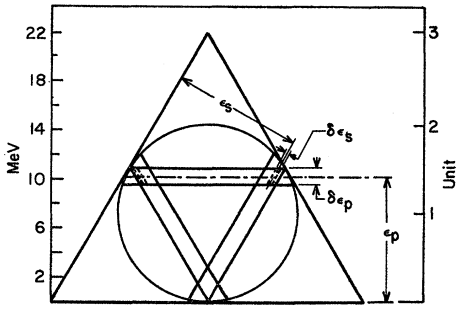

FIG. 5. Use of a Dalitz diagram to predict the expected coincidence ratio for random or "phase-space" breakup into three alphas.

[7] See, for example, *Experimental Nuclear Physics*, edited by E. Segrè (John Wiley & Sons, Inc., New York, 1953), Vol. 1.

In Fig. 5, the radius of the Dalitz circle is 7.26 MeV. The energy selectivity of the PSS requires that one of the α's lie within the range (9.55–10.95) MeV. Let subscript p refer to this alpha. The corresponding points are found only within three narrow strips whose total area is approximately

$$\frac{18\delta\epsilon_p}{T}\left(2+\frac{9}{T^2}\epsilon_p^2-\frac{6}{T}\epsilon_p\right)^{1/2}. \quad (4)$$

From Eq. (3), for a given ϵ_p one can calculate the energy spread in ϵ_s due solely to the angular spread $\delta\theta_{ps}$ which is subtended by the SSD;

$$\delta\epsilon_s=\tfrac{1}{2}mv_s\left\{v_p\sin\theta_{ps}\mp\frac{v_p^2\cos\theta_{ps}\sin\theta_{ps}}{[v_p^2\cos\theta_{ps}+4((T/m)-v_p^2)]^{1/2}}\right\}\delta\theta_{ps}. \quad (5)$$

Thus, the configuration points which represent the coincident events are found in the small dashed parallelograms whose total area is

$$36\sqrt{3}\delta\epsilon_s\delta\epsilon_p/T^2. \quad (6)$$

The alphas coincident with those detected by the PSS and having energies consistent with the angular range of the SSD are emitted in a conical shell of angular thickness $\delta\theta_{ps}$, subtending solid angle $2\pi\sin\theta_{ps}\delta\theta_{ps}$. If the solid angle subtended by the SSD is Ω_s the probability of capturing a coincident alpha by the SSD is

$$\Omega_s/2\pi\sin\theta_{ps}\delta\theta_{ps}. \quad (7)$$

Finally, from Eqs. (4), (6), and (7), the coincidence ratio as defined previously is

$$\frac{2\sqrt{3}\delta\epsilon_s}{T}\times\frac{1}{(2+9\epsilon_p^2/T^2-6\epsilon_p/T)^{1/2}}\times\frac{\Omega_s}{2\pi\sin\theta_{ps}\delta\theta_{ps}},$$

and using Eq. (5) we obtain for the predicted random coincidence rate Φ

$$\Phi=\frac{\Omega_s}{\pi T}\left(\frac{\frac{3}{2}m\epsilon_s}{2+9\epsilon_p^2/T^2-6\epsilon_p/T}\right)^{1/2}\times\left\{v_p\mp\frac{v_p^2\cos\theta_{ps}}{[v_p^2\cos^2\theta_{ps}+4((T/m)-v_p^2)]^{1/2}}\right\}. \quad (8)$$

Table III shows the predicted coincidence rates; the constants used in the calculation were

$$\Omega_s=3.4\times10^{-3}\text{ sr},\quad T=21.83\text{ MeV},\quad \epsilon_p=10.25\text{ MeV},$$

and ϵ_s is calculated from Eq. (3). The results are also indicated on Fig. 11.

The fact that the observed coincidence pattern differs widely from that predicted by uniform phase-space breakup shows clearly that the breakup is not random.

TABLE III. Predicted coincidence rates for random breakup and for a 6.4-MeV Be^8 level.

θ_s	θ_{ps}	Predicted coincidence rate Hyp. 1. Eq. (8) ($\times10^3$ sec^{-1})	Predicted coincidence rate Hyp. 2, Eq. (9) ($\times10^3$ sec^{-1})
321°	220°	1.28	1.48
311°	210°	1.42	1.67
301°	200°	1.53	1.81
291°	190°	1.60	1.89
281°	180°	1.63	1.92
271°	170°	1.60	1.89
261°	160°	1.53	1.81
251°	150°	1.42	1.67
241°	140°	1.28	1.48

However, the fact that the maximum of the peak in Fig. 1 is not at half the maximum energy available to any single alpha particle is in itself sufficient evidence against random breakup.

2. 6.4-MeV State Hypothesis

If one assumes a two-stage reaction of Eq. (2), in which the α_1 is captured by the PSS the coincidence distribution of the α_2 (or α_2') which is emitted by the recoiling Be^{8*} in the 6.4-MeV state and captured in the SSD is determined by the spin of the state and the relative angular momentum of the α_1+Be^{8*} system.

In discussing this and the following hypothesis, we will make appropriate changes in the notation for the angular positions of the detectors. We are now assuming two classes of alpha particles; α_1 arises from a recoil from a Be^{8*}, and α_2 or α_2' from a breakup of the recoiling Be^{8*}. At present, we are assuming that it is α_1 which is captured in the PSS, and has 10.25 MeV kinetic energy. Thus, in Eqs. (9) and the following discussion we use θ_1 for θ_p and θ_{12} for θ_{ps}.

If $J=0^+$, Be^{8*} decays into two alpha particles isotropically in its own frame. Then the coincidence distribution in the barycentric system is

$$\frac{\Omega_s Y(\theta_{12})}{n_0}=\frac{\Omega_s}{2\pi}\times\frac{[-\gamma\cos\theta_{12}+(1-\gamma^2\sin^2\theta_{12})^{1/2}]^2}{(1-\gamma^2\sin^2\theta_{12})^{1/2}}, \quad (9)$$

where

$$\gamma=\frac{\text{recoiling velocity of } Be^{8*} \text{ in the c.m. system}}{\text{velocity of } \alpha_2 \text{ in the beryllium system}}.$$

$Y(\theta_{12})/n_0$ is the coincidence rate per steradian, and Ω_s and θ_{12} are as defined previously. Equation (9) calculated in the range $140°<\theta_{12}<220°$ is shown in Table III and is indicated in Fig. 11.

If the 6.4-MeV state is a 2^+ state, the coincidence distribution is unchanged as long as the relative angular momentum of the α_1+Be^{8*} system is in an S state, because in this case there is no axis of quantization with respect to which the anisotropy of the α_2 particles can

arise. The assignment of $J=4^+$ to the hypothetical state at 6.4 MeV in Be^8 is unreasonable because the G-wave phase shift in alpha-alpha scattering is zero almost up to an incident laboratory energy of 14 MeV.[8]

3. 20-MeV State Hypothesis

In this hypothesis due to Coste and Marquez, we assume a two-stage reaction as in Eq. (2) but with the Be^{8*} in a highly excited state near 20 MeV. Thus, the α_1 carries very little energy in the barycentric system, and the α_2 and α_2' share the large excitation energy of the parent nucleus, Be^8. It is now the α_2 which carries the mean kinetic energy of 10.25 MeV in the barycentric system and is captured by the particle selection system. The α_2' is captured by the SSD, and in what follows under this hypothesis we shall consider θ_p identical with θ_2, and θ_{ps} with $\theta_{22'}$. The α_2' is expected to exhibit a unique coincidence distribution with a high intensity near $\theta_{22'}=180°$, since the two alphas are emitted from a Be^{8*} very nearly at rest in the barycentric system of the main reaction. Since the experimental results clearly show such a pattern, more detailed calculations of the predicted coincidences were carried out for this case than for the others. Figure 6 shows vectorial combinations of velocities in which the range of energies admitted by the PSS is included. The recoil velocity of Be^{8*} in the barycentric system, v_B, and the excitation X of the Be^{8*} with respect to two free alpha particles are connected as follows:

$$v_B=\left[\frac{2m(T-X)}{M(m+M)}\right]^{1/2},$$

where

$$T=2\delta_{\mathrm{Li}}-3\delta_\alpha+\tfrac{1}{2}E.$$

M is the mass of Be^8; the δ's represent atomic mass excesses in energy units and E is the energy of the incident Li^6 in the laboratory system.

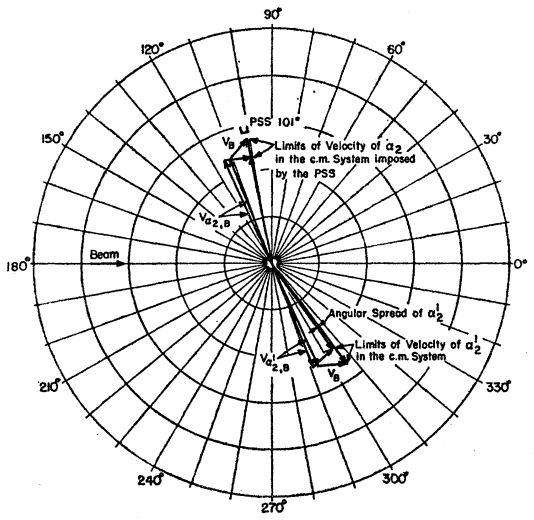

FIG. 6. Vector velocity diagram of the type used in calculating the double coincidences to be expected on the 20-MeV state theory.

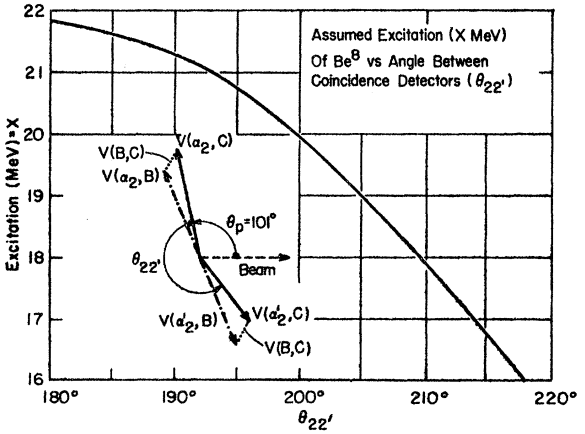

FIG. 7. It is assumed that the first alpha particle (not shown) recoils from a Be^8 nucleus retaining the excitation energy X MeV. The two breakup alphas (α_2,α_2') which follow have velocities corresponding to $\frac{1}{2}X$ with respect to their parent Be^8. The fact that the PSS system limited the mean energy of α_2 in the barycentric system to 10.25 MeV and fixed its angle defines the recoil of the Be^8, v(B,C); the angle $\theta_{22'}$ can then be calculated.

The particle selector system confines the energies of the α_2 particles it receives between 9.55 and 10.95 MeV in the barycentric system and their angles to 101° in that system. For a given excitation energy in Be^8, the velocity vector, v_B, of the recoiling Be^{8*} and the velocity vector, $v(\alpha_2,B)$, of the emitted α_2 particles in the beryllium system can be combined to produce a resultant vector which lies within the acceptable velocity range determined by the particle selection system. It is shown in Fig. 6 that this 1.4-MeV energy range accepted in the PSS causes an angular spread through which the coincident α_2' particles can be emitted. The maximum and the minimum angles of emission of the α_2' particles with respect to the α_2 particles in the barycentric system are tabulated in Table IV for assumed excitation energies of Be^8 from 16.8 MeV to the maximum available energy, 21.83 MeV (this is $T=2\delta_{\mathrm{Li}}-3\delta_\alpha+\frac{1}{2}E$). This table was

TABLE IV. Kinematical relationships for coincidence calculations. (See Fig. 6).

Postulated Be^8 excit. (MeV)	Min angle $\theta_{22'}$	Max angle $\theta_{22'}$	Detector position θ_s	$S(\theta_{2,2'})$
16.8	213°37′	215°06′	315°22′	0.026
18.0	208°56′	209°57′	309°57′	0.030
19.0	204°35′	205°09′	305°52′	0.036
20.0	199°33′	199°36′	300°35′	0.044
20.8	194°33′	194°34′	295°34′	0.040
21.2	190°15′	191°23′	291°53′	0.046
21.3	189°02′	190°28′	290°45′	0.052
21.4	187°38′	189°26′	289°22′	0.060
21.5	186°04′	188°18′	288°10′	0.063
21.6	183°44′	186°57′	286°20′	0.088
21.7	180°	184°45′	283°23′	0.222
21.8	180°	182°54′	282°27′	0.700
21.83	180°	180°	281°	1

compiled by postulating an excitation energy (column 1) and solving the analytical problem corresponding to the triangles in Fig. 6. The connection between the mean angle θ_{22}' and the postulated Be^8 excitation is shown in Fig. 7. Column 4 of Table IV shows the angle, θ_s, consistent with the mean angle θ_{22}'.

The vector diagram of Fig. 6 has rotational symmetry about the 101°–281° axis, and the vectors to the minimum and maximum angles θ_{22}' sweep out a conical shell into which the α_2''s are emitted. The factor $S(\theta_{22}')$ of column 5 of Table IV shows the fraction of these α_2's which were collected by the solid-state detector placed at θ_s.

We now introduce the excitation function of the hypothetical Be^{8*} resonance, of characteristic width Γ. We assume a Breit-Wigner function

$$P(X)=\frac{2/\pi\Gamma}{1+4(X-E_r)^2/\Gamma^2}, \tag{10}$$

with

$$\int_{-\infty}^{\infty} P(X)dX=1. \tag{11}$$

For any assumed E_r, the coincidence rate to be expected at any setting θ_s of the solid-state detector can be computed from

$$\Phi(\theta_{22}')=P(X)S(\theta_{22}')\Delta X. \tag{12}$$

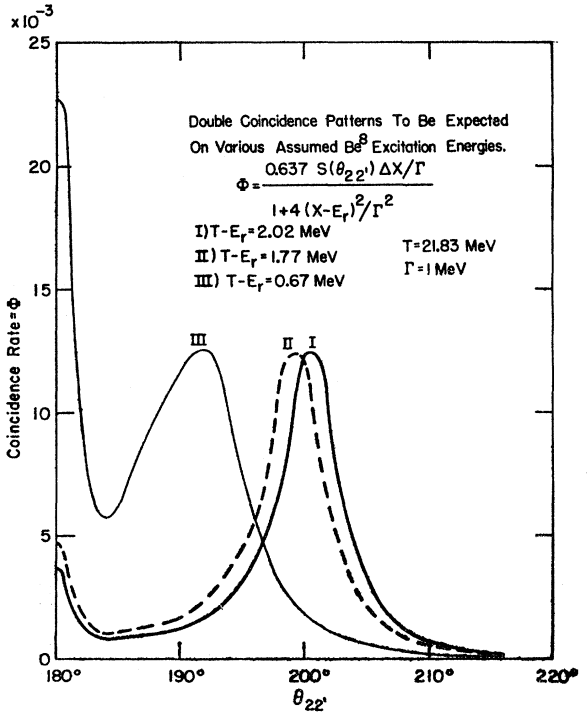

FIG. 8. The pattern is symmetrical about $\theta_{22}'=180°$. The coincidence maximum at 180° corresponds to $X=T$, meaning Be^8 breakup at rest in the barycentric system. The satellite peaks represent $X=E_r$, α_2 and α_2' being emitted from a Be^{8*} in motion in the barycentric system.

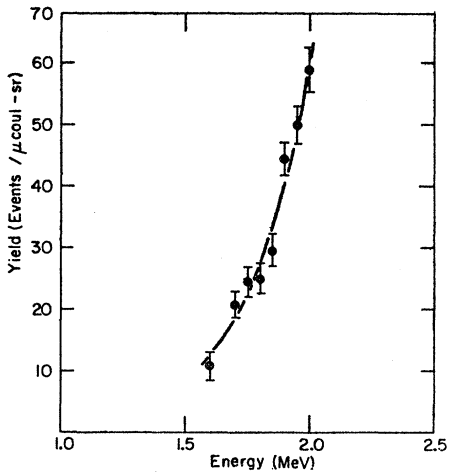

FIG. 9. Yield of the alpha particles recoiling from the ground state of Be^8 as a function of Li^6 bombarding energy on a thick LiF target. Taken at 90° (lab).

The excitation X for any θ_{22}' (or θ_s) can be read from the graph of Fig. 7. Since the SSD subtended an angle of 3°46′, the value of ΔX can be found for any θ_{22}' from Fig. 7 by considering this angular interval at the appropriate abscissa.

In order to explore the type of coincidence pattern predicted by Hypothesis 3, three calculations were carried out, one for each of three postulated E_r values in Be^8. The hypothetical states selected were 19.81, 20.06, and 21.16 MeV for Eq. (10). Following Temmer,[3] Γ was set at 1 MeV. These excitation energies are measured from the ground state of the system of two free alpha particles. Thus, the binding energy, 95 keV, of the ground state of Be^8 is added to the states in Be^8.

The 19.81-MeV state was derived from the spectrum in Fig. 1 assuming that the alpha particles which make up the maximum of the intense peak located at 10.25 MeV arise from a disintegration of Be^8 in which the α_2 and α_2' are emitted at right angles to the direction of motion of the recoiling Be^8. The 20.06 MeV was suggested by Temmer.[9] The 21.16 MeV was calculated by matching the coincidence rate at $\theta_{22}'=180°$ with the experimental results. The three coincidence curves are plotted in Fig. 8. It is seen that the maximum at $\theta_{22}'=180°$ and the satellite maxima are similar to those observed, as in Table II and Fig. 4, showing clearly[10] that a highly excited state of Be^8 is involved, as in Hypothesis 3.

The standard deviation in the coincidence experiment is rather large due to the low coincidence rate at each

[8] R. Nilson, W. K. Jentschke, G. R. Briggs, R. O. Kerman, and J. N. Snyder, Phys. Rev. **109**, 850 (1958).

[9] G. M. Temmer (private communication).

[10] This is contrary to the conclusion expressed in a previous note [Bull. Am. Phys. Soc. **7**, 549 (1962)]. In the first coincidence trials a source emitting both Li^7 and Li^6 ions was used, and the satellite peaks (Fig. 4) were not recognized in the data. The main coincidence peak at $\theta_{22}'=180°$ was erroneously ascribed to interference from the $p(Li^7,\alpha)\alpha$ reaction.

angle. The highest coincident count was 207 counts in a 2-h run, which has a standard deviation of 7%. The uncertainty in the angular position of the solid-state detector was ±5°.

C. Angular Distribution of the Alpha Particles Associated with the Be^8 Ground State, and Absolute Cross Sections

The relatively weak, highest energy group in the α spectrum of Fig. 1 corresponds to Be^8 being left in its ground state. The relative differential cross section for the group was taken at 18 angles which were transformed to the barycentric system.

The angular distribution was expressed in a series of Legendre polynomials,

$$Y(\theta)=Y_0\{1+\sum_1^3 A_{2l}P_{2l}(\cos\theta)\}. \quad (13)$$

The least-squares analysis as described by Rose[11] was carried out by a computer to the sixth-order Legendre polynomials. The weight factor for each point is the inverse of the square sum of the standard deviations for the yield and the monitor counts. Since the projectile and the target are identical, it was assumed that only the even terms should contribute to the angular distribution. The cross sections for barrier penetration between Li^6 and Li^6 were calculated according to the tables of Feshbach, Shapiro, and Weisskopf.[12]

Since the cross section for $l=3$ is[13] 1/20 of that for $l=0$, the sixth-order term in the Legendre expansion is expected to be small. The result of the least-squares analysis is the solid curve of Fig. 10.

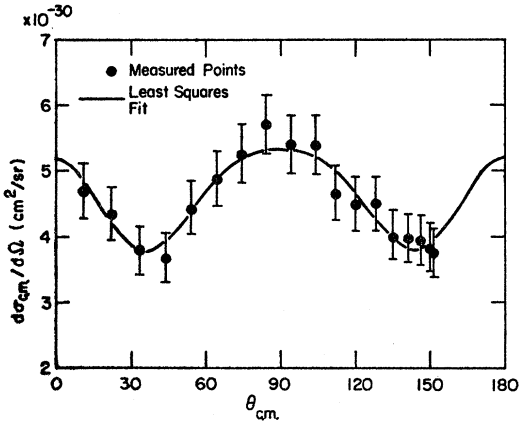

FIG. 10. Points show measured $d\sigma/d\Omega$ values for the ground-state alphas. The curve is the best fit in an expansion in cosines of even powers 0 to 6 inclusive.

[11] M. E. Rose, Phys. Rev. **91**, 610 (1953).
[12] H. Feshbach, M. M. Shapiro, and V. F. Weisskopf, Report NDA 15B-5, NYO 3070, of Nuclear Development Associates, Inc., White Plains, New York (unpublished).
[13] M. N. Huberman, M. Kamegai, and G. C. Morrison, Phys. Rev. **129**, 791 (1963); Table II. For "1.7" read 7.2.

TABLE V. Calculation of absolute differential cross section for ground-state alpha particles. [See Eq. (2) of Ref. 6.]

Incident Li^6 energy (laboratory)	2.0 MeV±0.8%
Yield of alpha particles	0.189 α's per μC (±8%)
Solid angle of acceptance at 90° (lab)	3.32×10^{-2} sr (±3%)
dY/dE at 2.0 MeV	240 per μC per MeV (±10%)
N_t	2.41×10^{19} Li^6 nuclei per mg LiF
Stopping power of LiF	3.3 MeV×cm²/mg±10%
$[d\sigma/d\Omega]_{c.m.}/[d\sigma/d\Omega]_{lab}$	1.012
$d\sigma/d\Omega$ at 98.7° c.m.; 2.0 MeV lab	5.3×10^{-30} cm²/sr (±15%)

The reduction of these relative differential cross sections to absolute values was accomplished by a measurement of the absolute cross section at 90° in the laboratory as has been described in HKM using Eq. (2) of that report. The excitation curve of the α_0 particles from a thick LiF target is shown in Fig. 9 and Table V shows values used in the computation of the absolute cross-section, including estimates leading to a possible ±15% error.

Expressed in absolute units, the constants of Eq. (13) are

$$Y_0=(4.65\pm0.05)\times10^{-30},$$
$$A_2=(-0.204\pm0.020),$$
$$A_4=(0.203\pm0.030),$$
$$A_6=(0.116\pm0.032).$$

The total cross section was obtained by integrating the differential cross section:

$$\sigma=(5.85\pm0.88)\times10^{-29}\ \text{cm}^2.$$

IV. DISCUSSION

The examination of Fig. 4 in the light of the three hypotheses reveals convincing evidence that the mechanism of the third hypothesis plays a preponderant role in this reaction. Thus, we assign the principal α peak of Fig. 1 to breakup alphas from a Be^8 excited state near 20 MeV, and from our spectra taken at various angles and the absolute cross-section result on the α's from the ground state the estimated total cross section for the reaction which proceeds through the 20-MeV Be^8 state is

$$\sigma=13\times10^{-28}\ \text{cm}^2\pm20\%$$
for 2.0-MeV (lab) Li^6 bombardment.

This is 23 times the probability that the reaction will proceed through the ground state of Be^8.

If an essential feature of the compound nucleus mechanism is that the intermediate stage must live long enough for statistical distribution of the reaction energy among the nucleons present it is difficult to use it to explain this relatively large yield through the exit channels in which the 20-MeV state is involved. An important factor in the cross section should be the penetration of the Coulomb barrier from the inside by

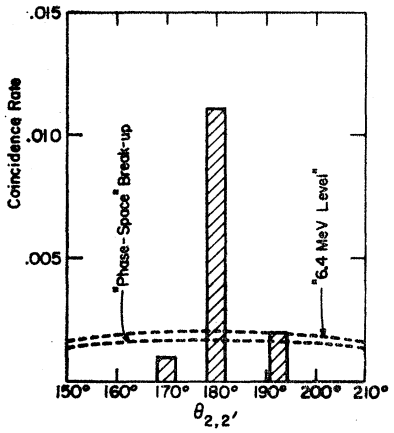

FIG. 11. The observed coincidence ratios grouped in the form of a histogram whose angular width is the angle subtended by the solid-state coincidence detector (3°46′). The absence of coincidences between the satellites and the central peak is real; not due to lack of observations. Predicted patterns from discarded hypotheses are indicated.

the produced charged particles, which are Be^8 and α. The velocity of separation of these two products is 7.2×10^8 cm/sec in the 20-MeV channels and 5.4 times this or 3.9×10^9 cm/sec in the ground-state channels, which should lead to a much greater penetration factor and cross section for the latter; opposite to the effect observed. However, the angular momentum of the 20-MeV Be^8 state may be greater than that of the ground state, which corresponds to $l=0$. Thus, the relative angular momentum involved in the Be^8-alpha separation may be less in the 20-MeV channel than in the ground-state channel, which would affect the yield from the 20-MeV channels, but not by a sufficiently large factor, for our angular distribution analysis has shown that a Be^8-alpha separation with $l=0$ is prominent even in the ground-state alphas.

According to the Temmer theory and the interpretation advanced by the Saclay group, the reaction which leads to the 20-MeV state may be best interpreted as a cluster reaction. Namely, one lithium-6 nucleus captures a deuteron cluster of the other lithium-6 nucleus to form a kind of threshold resonance state as described by Baz[14] and Inglis.[15]

If a one-level Breit-Wigner formula is assumed, one can estimate the excitation energy and its width in Be^8 from the data on the coincidence distribution in Fig. 4. The calculation is done in the following manner. The sharp peak at $\theta_{22'}=180°$, arises from the α_2 and the α_2' which are emitted by a Be^{8*} stationary in the barycentric system. On the other hand, the satellite peaks located at $\theta_{22'}=192°$ and 169°, result from the high probability of occupation by Be^8 of a characteristic excitation energy, E_r. Thus, the angular position of the satellite peaks in the coincidence data will serve to locate the state in Be^8 by the use of Fig. 7 and the ratio of the sharp peak at $\theta_{22'}=180°$ to the satellite peaks will enable us to calculate the width, Γ.

As a first step, the coincidence data of Table II is plotted in the form of a histogram, Fig. 11. The $192\frac{1}{2}°$ group resulted from the excitation energy of 21.12 MeV according to Fig. 7. The incident beam suffers an effective energy loss of 160 keV in the target so that in the barycentric system the kinetic energy is reduced by 80 keV. By subtracting the effective energy loss and the binding energy of Be^8, 95 keV, from 21.12 MeV, the state in question is calculated to be (20.95±0.30) MeV. This is somewhat higher but may be the 19.96-MeV state suggested by Temmer.

The width, Γ, is obtained in the following manner. From Eq. (12)

$$\Phi(180°)=\frac{0.637\Gamma^{-1}\Delta X_{180°}}{1+4(21.83-E_r)^2/\Gamma^2}S(180°), \qquad (14)$$

where $E_r=21.12$ MeV, $\Delta X_{180°}=0.10$ MeV, [see explanation following Eq. (12)] and $S(180°)=1$, i.e., at $\theta_{22'}=180°$ the α_2' particles occupy a solid angle less than subtended by the SSD. For the satellite at $\theta_{22'}=192.5°$

$$\Phi(192.5°)=0.637\Gamma^{-1}\Delta X_{192.5°}S(192.5°), \qquad (15)$$

since the Be^8 is excited to the center of the resonance.

$$\Delta X_{192.5}=0.32 \text{ MeV}, \quad \text{and} \quad S(192.5)=0.043.$$

From Fig. 11, we take the observed ratio

$$\Phi(192.5°)/\Phi(180°)=0.182,$$

and from Eqs. (14) and (15) we can calculate the total width

$$\Gamma=3.4 \text{ MeV}.$$

The total cross section at or near the resonance energy may be written[16] as

$$\sigma=\frac{2J+1}{(2s+1)(2I+1)}\times\frac{4\pi\lambda\!\!\!^{-2}\Gamma_\alpha\Gamma_d}{\Gamma^2}, \qquad (16)$$

where J is the channel spin; s is the projectile spin; I is the target spin; $\lambda\!\!\!^{-}$ is the De Broglie wavelength divided by 2π for the relative motion of the deuteron-lithium system; Γ_d is the deuteron capture width; and Γ_α is the alpha decay width. Considering the effective energy loss in the target material, the De Broglie wavelength for 1.9-MeV incident energy is calculated to be

$$\lambda\!\!\!^{-}=5.66\times10^{-13} \text{ cm}.$$

Although the deuteron capture width is not obvious, one can make a crude estimate. The deuteron resonance width for $Li^6(d,d')Li^{6*}$ is[17] 25 keV, where the excitation energy of Li^6 is 2.2 MeV. Thus, the deuteron capture width in the reaction with which we are concerned must be less than 25 keV because in this case the deuteron cluster must escape from the parent nucleus, Li^6, to be captured by a target Li^6.

[14] A. I. Baz, in *Advances in Physics*, edited by N. F. Mott (Taylor and Francis, Ltd., London, 1959), Vol. 8, p. 349.
[15] D. R. Inglis, Nucl. Phys. **30**, 1 (1962).
[16] J. M. Blatt and L. C. Biedenharn, Rev. Mod. Phys. **24**, 258 (1952).
[17] F. Ajzenberg and T. Lauritsen, Nucl. Phys. **11**, 1 (1959).

Substituting into Eq. (16)

$$J=2^+,$$
$$s=I=1,$$
$$\Gamma=3.4 \text{ MeV},$$
$$\Gamma_d<25 \text{ keV},$$

and

$$\sigma=13\times10^{-28} \text{ cm}^2,$$

we obtain

$$\Gamma_\alpha>260 \text{ keV}\pm35\%.$$

A. Angular Distribution

Although the observed angular distribution[18] of the ground state alphas was formally calculated out to polynomials involving $\cos^6\theta$, it is probable that there is no sound evidence for terms higher than $l=2$ for the following reasons. It was found that this angular distribution could be well fitted by only two terms,

$$Y(\theta)=Y_0(1+\sum_1^2 A_{2L}P_{2L}),$$

where $Y_0=(4.556\pm0.049)\times10^{-30}$, $A_2=-0.200\pm0.020$, $A_4=0.239\pm0.029$. The total square deviation of the least-squares analysis is defined by

$$\text{SD}=\sum_i W(\theta_i)[y(\theta_i)-Y(\theta_i)]^2,$$

where $W(\theta_i)$ is the weight factor at θ_i, $y(\theta_i)$ is the experimental value and $Y(\theta_i)$ is the calculated value. The total square deviations for the three Legendre functions and the two Legendre functions, respectively, are

$$\text{SD}_3=2.56\times10^{-58}$$
$$\text{SD}_2=2.72\times10^{-58}$$

so that

$$[\text{SD}_2]^{1/2}[\text{SD}_3]^{-1/2}=1.03.$$

Thus, there is only 3% difference in the total deviation. The apparent contribution from $P_6(\cos\theta)$ term probably arises from the assignment of the incorrect weight factors to the experimental points. The determination of the weight factors strictly from the statistical errors as it was done here is not exactly correct. The reliability of the observation at each point must be taken into consideration.

Probably, the ground state of Be^8 is formed through an intermediate compound nucleus. If it is correct that the maximum complexity of the angular distribution of the emitted alpha particles is $P_4(\cos\theta)$ which corresponds to $l=2$, this is the maximum relative orbital angular momentum of the incident particles. Since the cross section of the formation of a compound nucleus for Li^6+Li^6 is dominated[19] at our bombarding energies by $l=0$, 1, and 2, the observed angular distribution is consistent with theoretical predictions.[20]

ACKNOWLEDGMENTS

The author wishes to thank Professor S. K. Allison for his sponsorship and guidance throughout this work. Also, he is indebted to Dr. S. Johnson of the Enrico Fermi Institute and Dr. B. Garbow of Argonne National Laboratory for their valuable discussions on the computer programming. The Computer Institute of the University of Chicago, particularly the computer librarian, R. Brunke, was most helpful in the analysis of data. B. Sahai read the manuscript and provided many helpful suggestions. Finally, the author wishes to thank J. Erwood, L. Palmer, and W. Tomasek for their technical assistance.

[18] This angular distribution agrees qualitatively with that found under the same conditions by Coste [Compt. Rend. **255**, 2750 (1962)]. However Coste's ratio for the maximum at 90° to the minima at 40° and 140° is about 2.1; the present value is 1.5.

[19] See Table II of Ref. 6.

[20] L. Wolfenstein, Phys. Rev. **82**, 690 (1951).